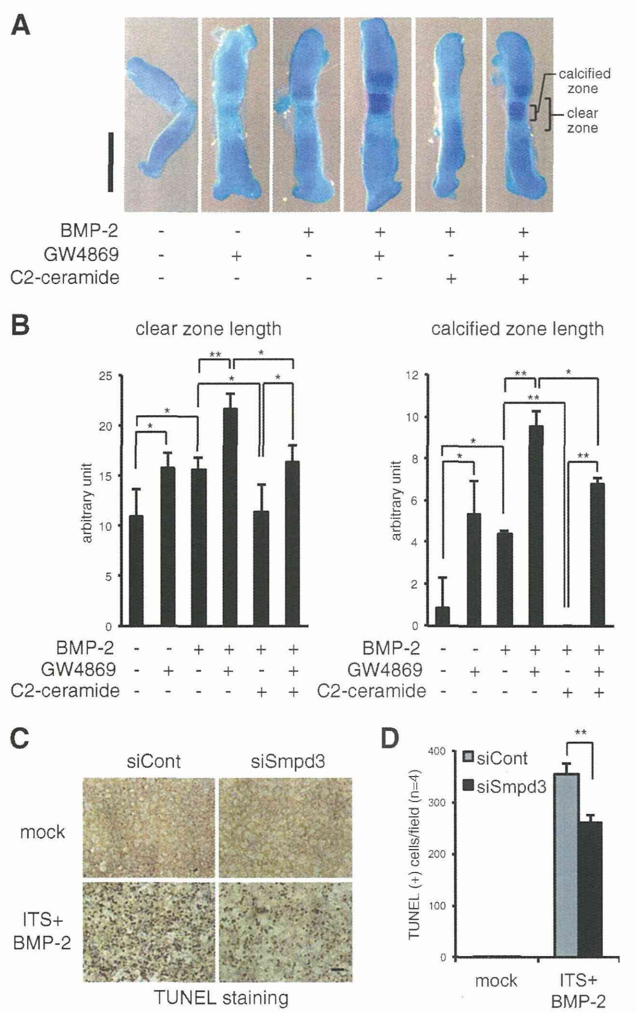

FIGURE 6. **Blocking of nSMase2 function by GW4869 promotes, whereas mimicking the function by C_2-ceramide suppresses, hypertrophic maturation of chondrocytes in *ex vivo* mouse cartilage rudiment culture and loss of *Smpd3* decreased apoptosis of ATDC5 chondrocytes.** *A* and *B*, metatarsal bones from E16.5 mouse embryo were cultured with BMP-2 (300 ng/ml) in combination with GW4869 (1 μM) and/or C_2-ceramide (10 μM) for 3 days. The cartilage matrix was stained with Alcian blue, and the chondrocyte matrix calcified by mature hypertrophic chondrocytes was stained by alizarin red (*A*). The *clear zone* represents hypertrophic chondrocytes. *Scale bar*, 500 μm. The length of the hypertrophic clear zone and the *calcified zone* were measured ($n = 4$) (*B*). *C* and *D*, ATDC5 cells were transfected with control siRNA (*siCont*) or *Smpd3* siRNA (*siSmpd3*) for 16 h and further stimulated by ITS supplement and BMP-2 (300 ng/ml) for 6 days. Apoptotic cells were visualized by TUNEL immunoperoxidase staining (*C*). *Scale bar*, 300 μm. The number of apoptotic cells was counted ($n = 4$) (*D*). *, $p < 0.05$; **, $p < 0.01$.

of BMP-2 treatment was negated by the addition of LY294002 or MK2206, suggesting that the *Has2* gene is under the control of the PI3K or Akt pathway, respectively (Fig. 7*G*). These data suggest that Has2 plays a role in the *Smpd3*/nSMase2-mediated inhibition of chondrocyte maturation via PI3K-Akt signaling.

DISCUSSION

Previous reports had suggested that Smpd3/nSMase2 may have a crucial role in *in vivo* chondrogenesis (36–38). We observed a moderate level of *Smpd3* expression in the brains of adult mice (Fig. 1*I*), consistent with the finding that *Smpd3*$^{-/-}$ mice showed a defect in the hypothalamus-pituitary growth axis, which likely accounted for the dwarfism (37). However, the enlarged hypertrophic zone and retarded apoptosis in the chondrocytes of mutant mice cannot be explained by the reduced production of growth hormone and IGF (37). In this study, we present evidence for a cell-autonomous role of the nSMase-ceramide axis in regulating Akt signaling and the subsequent chondrogenic marker expression and differentiation. The induction of *Smpd3* by BMP-2 was a common feature among the tested chondrogenic cells, including primary articular chondrocytes, but *Smpd3* did not seem to be a direct target of the BMP-Smad pathway. Its coding protein, nSMase2, was dominant in mature hypertrophic chondrocytes *in vivo* (Fig. 1*J*), with an expression pattern resembling that of Runx2, whereas the loss of Runx2 suppressed expression of *Smpd3* (Fig. 2, *C, D* and *F*). Taken together with the evidence that Runx2 directly interacts with and activates the promoter of *Smpd3* in C2C12 myoblasts (39), Runx2 seems to be mainly responsible for the spatiotemporal expression of *Smpd3* in chondrocytes, in concert with BMP signaling. In addition, it should be noted that the maximum expression of *Smpd3*/nSMase2 *in vivo* was observed in bone tissue, where Runx2 is highly expressed. So far, the molecular mechanism by which BMP-2 increases Runx2-dependent expression of *Smpd3* remains unclear. It is likely that a mechanism similar to that of *Col10a1* gene induction, in which BMP-activated Smads interact with Runx2 to enhance the *Col10a1* promoter-activating ability of Runx2 to drive chondrocyte maturation (13), may take place on the *Smpd3* promoter.

PI3K and its downstream Akt are activated by a large number of receptors, but most notably by tyrosine kinases, such as the IGF-1 receptor. The majority of published studies suggest that PI3K or Akt signaling is required for normal hypertrophic cell maturation and endochondral bone growth during cartilage development (51, 54, 55), although the precise molecular mechanisms for this remain unclear. We demonstrated that the loss

FIGURE 5. **Blocking the Akt or PI3K pathway negates the *Smpd3* siRNA-mediated acceleration of chondrogenesis initiated by BMP-2 in ATDC5 cells.** *A*, ATDC5 cells were transfected with control siRNA (*siCont*) or *Smpd3* siRNA (*siSmpd3*) for 16 h and stimulated by BMP-2 (300 ng/ml) with or without MK2206 at the indicated concentrations (micromolar) for 6 days. Expression of *Smpd3, Acan, Col2a1*, and *Col10a1* was evaluated by quantitative RT-PCR. *B*, ATDC5 cells were transfected with control siRNA (*siCont*) or *Smpd3* siRNA (*siSmpd3*) for 16 h, and then cultured in the presence of BMP-2 (300 ng/ml) with or without MK2206 (10 μM) for 9 days. Alcian blue staining was performed. *Scale bar*, 300 μm. *C*, ATDC5 cells were transfected with control siRNA (*siCont*) or *Smpd3* siRNA (*siSmpd3*) for 16 h and stimulated by BMP-2 (300 ng/ml) with or without rapamycin at the indicated concentrations (micromolar) for 3 days. Expression of *Smpd3* and *Col10a1* was evaluated by quantitative RT-PCR. *D*, ATDC5 cells were transfected with control siRNA (*siCont*) or *Smpd3* siRNA (*siSmpd3*) for 16 h and stimulated by BMP-2 (300 ng/ml) for 24 h, and then immunoblotted for the indicated antibodies. Tubulin served as a loading control. *E*, ATDC5 cells were transfected with control siRNA (*siCont*) or *Smpd3* siRNA (*siSmpd3*) for 16 h and further stimulated by BMP-2 (300 ng/ml) with or without LY294002 at the indicated concentrations (μM) for 6 days. Expression of *Smpd3, Acan, Col2a1*, and *Col10a1* was evaluated by quantitative RT-PCR analysis. *F*, mouse primary chondrocytes were transfected with control siRNA (*siCont*) or *Smpd3* siRNA (*siSmpd3*) for 16 h, and were further stimulated by BMP-2 (300 ng/ml) with or without LY294002 (*LY*, 25 μM), MK2206 (*MK*, 5 μM), or rapamycin (*Rp*, 0.5 μM) for 7 days. Expression of *Smpd3, Acan, Col2a1*, and *Col10a1* was evaluated by quantitative RT-PCR analysis. *, $p < 0.05$; **, $p < 0.01$; *n.s.*, not significant.

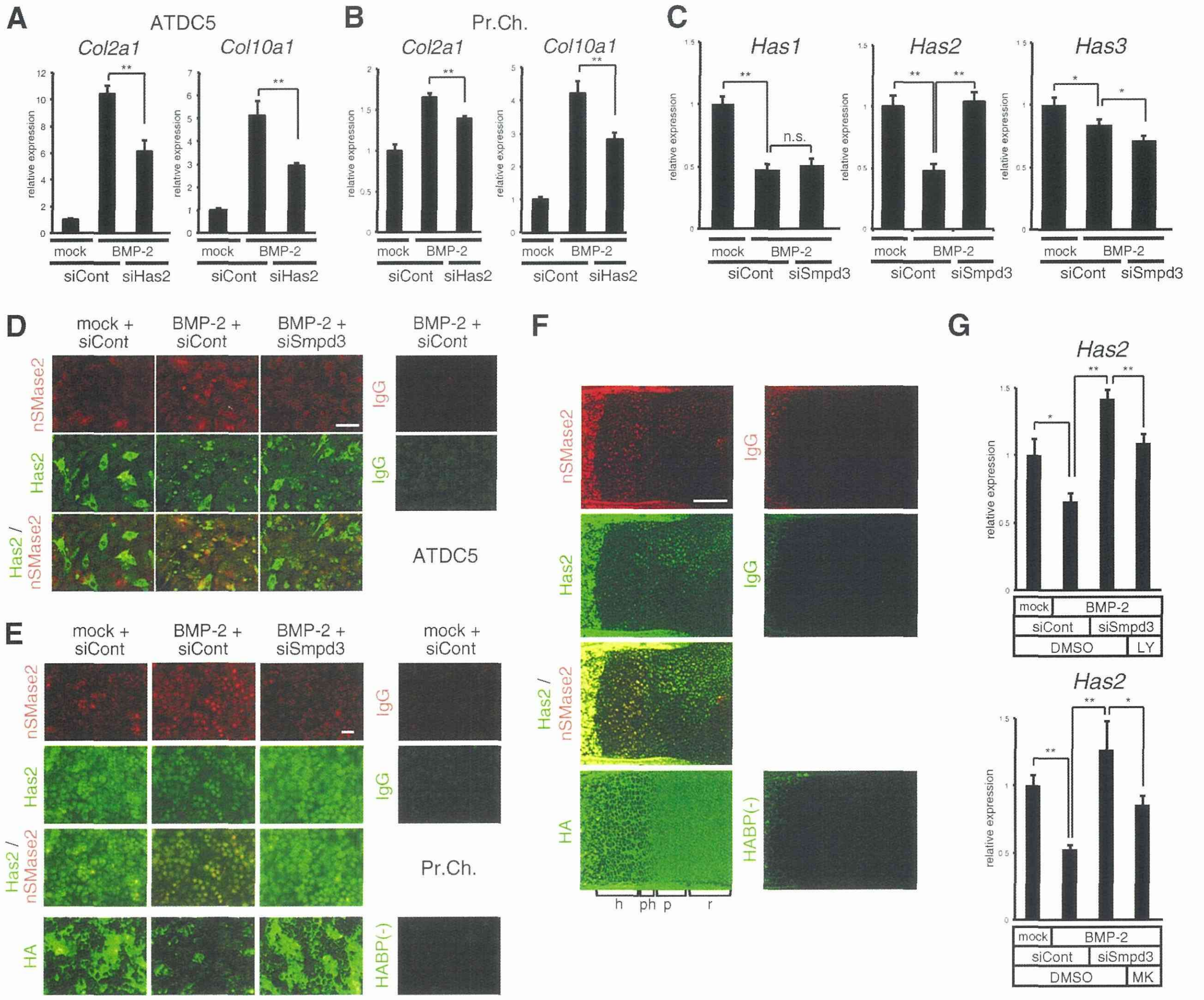

FIGURE 7. **Expression of Has2 is suppressed by nSMase2 via the PI3K or Akt pathway in ATDC5 cells, whereas localization of nSMase2 and Has2 is mutually exclusive in the growth plate cartilage of mouse embryo.** *A* and *B*, ATDC5 cells (*A*) or mouse primary chondrocytes (*B*) were transfected with control siRNA (*siCont*) or *Has2* siRNA (*siHas2*) for 16 h and then treated with BMP-2 (300 ng/ml) for 6 days. Quantitative RT-PCR analysis was performed for *Col2a1* and *Col10a1*. *C*, ATDC5 chondrocytes were transfected with control siRNA (*siCont*) or *Smpd3* siRNA (*siSmpd3*) for 16 h and then treated with BMP-2 (300 ng/ml) for 6 days. Quantitative RT-PCR analysis was performed for *Has1*, *Has2*, and *Has3*. *D*, immunofluorescence for nSMase2 or Has2 was performed in ATDC5 chondrocytes. IgG was used as negative control. *Scale bar*, 50 μm. *E*, immunofluorescence for nSMase2 or Has2 was performed on mouse primary chondrocytes. Biotin-conjugated hyaluronan-binding protein (*HABP*) and Alexa Fluor 488-conjugated streptavidin were applied to detect hyaluronan. IgG was the negative control. *Scale bar*, 50 μm. *F*, expression of nSMase2 or Has2 in mouse E17.5 humerus cartilage was evaluated by immunofluorescence. Biotin-conjugated HA-binding protein and Alexa Fluor 488-conjugated streptavidin were used to detect hyaluronan. IgG was the negative control. *r*, resting chondrocytes; *p*, proliferating chondrocytes; *ph*, prehypertrophic chondrocytes; *h*, hypertrophic chondrocytes. *Scale bar*, 250 μm. *G*, ATDC5 cells were transfected with control siRNA (*siCont*) or *Smpd3* siRNA (*siSmpd3*) for 16 h and further stimulated by BMP-2 (300 ng/ml) with or without LY294002 (*LY*, 1 μM) or MK2206 (*MK*, 1 μM) for 6 days. Expression of *Has2* was evaluated by quantitative RT-PCR analysis. *, $p < 0.05$; **, $p < 0.01$; *n.s.*, not significant.

or gain of *Smpd3*/nSMase2 function in chondrocytes increased or decreased the phosphorylation of both PI3K and Akt, respectively. In an RTK signaling antibody array, only phosphorylation of Akt and rpS6 was strengthened by the loss of *Smpd3* (Fig. 4*A*), demonstrating their specificity as downstream targets of nSMase2. Importantly, the increase in Akt phosphorylation was induced by the addition of BMP-2 and not by ITS alone (Fig. 4, *A*, *D* and *E*). A similar enhancement in the phosphorylation of Akt was observed within 1 h of BMP-2 application in gastric cancer cells, although the precise mechanism by which the BMP-2 signaling pathway induced Akt activity was unclear (56). We expect the Akt pathway to take part in BMP-2-induced chondrogenesis because this pathway promotes chondrocyte differentiation.

The GW4869-mediated blockade of nSMase2 function accelerated differentiation of ATDC5 chondrocytes, as well as hypertrophic conversion and calcification of chondrocytes, in bone *ex vivo* culture; both phenotypes were cancelled by application of C_2-ceramide (Figs. 3*C* and 6, *A* and *B*). nSMase2 hydrolyzes the phosphodiester bond of the membrane sphingolipid sphingomyelin to yield ceramide and phosphocholine (57). Ceramides have been shown to reduce the level of Akt phosphorylation by activating protein phosphatase 2A (PP2A) (58). The phosphorylation level of PP2A in *fro*/*fro* fibroblasts is

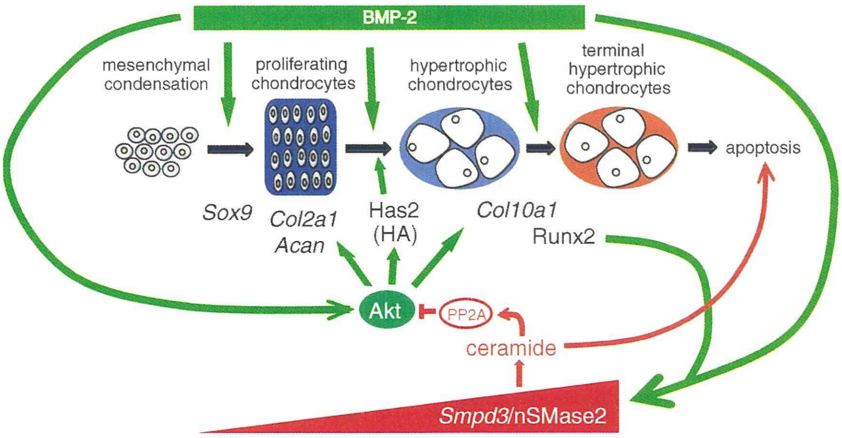

FIGURE 8. **Proposed model for the negative or positive regulation of chondrocyte maturation or apoptosis by *Smpd3*/nSMase2, respectively.** BMP-2 promotes chondrogenesis by multiple pathways, including activation of Akt signaling and the subsequent induction of Has2. During chondrocyte maturation, up-regulated Runx2 induces *Smpd3* in concert with BMP signaling. nSMase2 releases ceramide, which activates PP2A to dephosphorylate Akt. This blockade of the Akt pathway interferes not only with chondrocyte maturation but also with Has2-mediated production of HA.

reduced (50). Taken together, in the maturing phase of chondrogenesis, BMP-2-induced nSMase2 is thought to release ceramide, which in turn activates PP2A to inactivate Akt and the subsequent chondrogenic molecular cascades (Fig. 8). Thus, the *Smpd3*/nSMase2-ceramide axis negatively regulates BMP-2-induced activation of the Akt pathway through a negative feedback mechanism.

nSMase2 is one of the major intracellular regulators of sphingolipids, and many reports have implicated nSMase2 activation in ceramide-mediated apoptosis (49, 59–61). Sphingomyelinase-released ceramide is essential for the clustering of the death receptors CD95 or DR5 in membrane rafts to trigger apoptosis (62, 63). Indeed, silencing of *Smpd3* in mature ATDC5 chondrocytes reduced the number of apoptotic cells (Fig. 6, *C* and *D*), suggesting that delayed apoptosis in *fro*/*fro* cartilage was a cell-autonomous effect of the loss of function of nSMase2 (36). Because apoptosis of terminally matured hypertrophic chondrocytes is a crucial step in the transition of chondrogenic stage to the bone formation stage in the endochondral ossification system, *Smpd3*/nSMase2 probably plays a key role in regulating the timing of osteogenesis onset.

HA is a linear high molecular weight glycosaminoglycan and is composed of disaccharide repeats of glucuronic acid and *N*-acetylglucosamine. It is produced in the plasma membrane by three hyaluronan synthases (Has1–3); Has2 is the crucial hyaluronan synthase involved in the endochondral ossification process (53). The Akt-rpS6 pathway is important in the expression of *Has2* in MCF-7 breast cancer cells (64), although nSMase2 suppresses production of Has2 via inactivation of Akt in mouse dermal fibroblasts (50). In chondrocytes, Has2 expression was decreased by BMP-2 stimulation and was then recovered by silencing of *Smpd3*, demonstrating the importance of BMP-induced *Smpd3*/nSMase2 in the suppression of Has2 (Fig. 7, *C–E*). Because an inhibitor compound for PI3K or Akt cancelled this effect (Fig. 7*G*), *Has2* expression is also considered to be under the control of PI3K-Akt signaling. *In vivo*, expression of Has2 was diminished in hypertrophic chondrocytes, whereas nSMase2 was strongly expressed in the same cells (Fig. 7*F*). Taken together, these results indicate that Has2 is another mediator of *Smpd3*/nSMase2-induced inhibition of the hypertrophic maturation of chondrocytes, downstream of Akt signaling (Fig. 8).

Studies of articular cartilage suggest that ceramide plays a role in cartilage degeneration and the disruption of cartilage matrix homeostasis to decrease the levels of type II collagen (65, 66). Farber disease, in which a lack of ceramidase causes excess ceramide accumulation within the cartilage and bone, is associated with arthritis-like joint degeneration (67). Moreover, tumor necrosis factor α (TNFα), a proinflammatory cytokine that is widely implicated in the pathogenesis of arthritic diseases (68), can increase the level of ceramide through hydrolysis of the cell membrane lipid sphingomyelin by endosomal acidic and membrane-bound neutral sphingomyelinases (69). In chondrocytes, we observed a decrease of *Col2a1* expression by induction of C^2-ceramide or *Smpd3*-expressing adenovirus. Conversely, *Smpd3* knock-out mice showed an enlarged hypertrophic zone in the growth plate of the joints and, in adulthood, a severe OA-phenotype with osteophytes in the knee joint (38). Similarly, in chondrocytes, we observed increase of hypertrophic phenotype (*Col10a1*) by induction of *Smpd3* siRNA. Accordingly, an excess level of nSMase2 leads to the degradation of cartilage matrix proteins, whereas loss of nSMase2 introduces a hypertrophic change in chondrocytes, and both circumstances may result in the progression of OA. Therefore, the expression of *Smpd3*/nSMase2 must be fine-tuned to maintain cartilage homeostasis that is, at least in part, controlled by Runx2 and BMP signaling.

In the case of cartilage regenerative medicine, pharmacological manipulation of steps of the nSMase2-ceramide-PP2A-Akt pathway may improve the efficiency and quality of generated tissues. As an indication, it is noteworthy that we could manipulate hypertrophic conversion and calcification in *ex vivo* cartilage rudiment culture using combinations of BMP-2, GW4869, and C_2-ceramide (Fig. 6, *A* and *B*).

In summary, our study has provided a cell-autonomous pivotal role for *Smpd3*/nSMase2 in determining the rate of chondrocyte maturation in chondrocytes. As illustrated in Fig. 8, BMP-2 accelerates general chondrogenesis through multiple approaches, including activation of the Akt pathway, which involves induction of *Has2* and a subsequent production of HA. Meanwhile, increased Runx2 in maturating chondrocytes induces *Smpd3* in concert with BMP-2. nSMase2, coded by *Smpd3*, releases ceramide from the cell membrane to activate PP2A, which in turn dephosphorylates Akt. This inactivation of the Akt pathway suppresses not only chondrocyte differentiation and subsequent maturation but also production of HA via Has2. We propose that *Smpd3*/nSMase2 is a molecular target in cartilage and bone medicine that constitutes a negative feedback loop in BMP-induced chondrogenesis.

Acknowledgments—Human chondrocyte C28/I2 was kindly provided by Dr. Mary Goldring. We gratefully acknowledge the technical assistance of Hui Gao.

REFERENCES

1. Bi, W., Deng, J. M., Zhang, Z., Behringer, R. R., and de Crombrugghe, B. (1999) Sox9 is required for cartilage formation. *Nat. Genet.* **22,** 85–89
2. Akiyama, H., Chaboissier, M. C., Martin, J. F., Schedl, A., and de Crombrugghe, B. (2002) The transcription factor Sox9 has essential roles in successive steps of the chondrocyte differentiation pathway and is required for expression of Sox5 and Sox6. *Genes Dev.* **16,** 2813–2828
3. Provot, S., and Schipani, E. (2005) Molecular mechanisms of endochondral bone development. *Biochem. Biophys. Res. Commun.* **328,** 658–665
4. Enomoto, H., Enomoto-Iwamoto, M., Iwamoto, M., Nomura, S., Himeno, M., Kitamura, Y., Kishimoto, T., and Komori, T. (2000) Cbfa1 is a positive regulatory factor in chondrocyte maturation. *J. Biol. Chem.* **275,** 8695–8702
5. Zheng, Q., Zhou, G., Morello, R., Chen, Y., Garcia-Rojas, X., and Lee, B. (2003) Type X collagen gene regulation by Runx2 contributes directly to its hypertrophic chondrocyte-specific expression *in vivo*. *J. Cell Biol.* **162,** 833–842
6. Kronenberg, H. M. (2003) Developmental regulation of the growth plate. *Nature* **423,** 332–336
7. Miyazono, K., Maeda, S., and Imamura, T. (2005) BMP receptor signaling: transcriptional targets, regulation of signals, and signaling cross-talk. *Cytokine Growth Factor Rev.* **16,** 251–263
8. Guo, X., and Wang, X. F. (2009) Signaling cross-talk between TGF-β/BMP and other pathways. *Cell Res.* **19,** 71–88
9. Pogue, R., and Lyons, K. (2006) BMP signaling in the cartilage growth plate. *Curr. Top. Dev. Biol.* **76,** 1–48
10. Hatakeyama, Y., Tuan, R. S., and Shum, L. (2004) Distinct functions of BMP4 and GDF5 in the regulation of chondrogenesis. *J. Cell. Biochem.* **91,** 1204–1217
11. Haas, A. R., and Tuan, R. S. (1999) Chondrogenic differentiation of murine C3H10T1/2 multipotential mesenchymal cells: II. Stimulation by bone morphogenetic protein-2 requires modulation of N-cadherin expression and function. *Differentiation* **64,** 77–89
12. Fujii, M., Takeda, K., Imamura, T., Aoki, H., Sampath, T. K., Enomoto, S., Kawabata, M., Kato, M., Ichijo, H., and Miyazono, K. (1999) Roles of bone morphogenetic protein type I receptors and Smad proteins in osteoblast and chondroblast differentiation. *Mol. Biol. Cell* **10,** 3801–3813
13. Leboy, P., Grasso-Knight, G., D'Angelo, M., Volk, S. W., Lian, J. V., Drissi, H., Stein, G. S., and Adams, S. L. (2001) Smad-Runx interactions during chondrocyte maturation. *J. Bone Joint Surg. Am.* **83,** S15–S22
14. Valcourt, U., Gouttenoire, J., Moustakas, A., Herbage, D., and Mallein-Gerin, F. (2002) Functions of transforming growth factor-β family type I receptors and Smad proteins in the hypertrophic maturation and osteoblastic differentiation of chondrocytes. *J. Biol. Chem.* **277,** 33545–33558
15. Tsumaki, N., Nakase, T., Miyaji, T., Kakiuchi, M., Kimura, T., Ochi, T., and Yoshikawa, H. (2002) Bone morphogenetic protein signals are required for cartilage formation and differently regulate joint development during skeletogenesis. *J. Bone Miner. Res.* **17,** 898–906
16. Yoon, B. S., Ovchinnikov, D. A., Yoshii, I., Mishina, Y., Behringer, R. R., and Lyons, K. M. (2005) Bmpr1a and Bmpr1b have overlapping functions and are essential for chondrogenesis *in vivo*. *Proc. Natl. Acad. Sci. U.S.A.* **102,** 5062–5067
17. Retting, K. N., Song, B., Yoon, B. S., and Lyons, K. M. (2009) BMP canonical Smad signaling through Smad1 and Smad5 is required for endochondral bone formation. *Development* **136,** 1093–1104
18. Volk, S. W., Luvalle, P., Leask, T., and Leboy, P. S. (1998) A BMP-responsive transcriptional region in the chicken type X collagen gene. *J. Bone Miner. Res.* **13,** 1521–1529
19. Kempf, H., Ionescu, A., Udager, A. M., and Lassar, A. B. (2007) Prochondrogenic signals induce a competence for Runx2 to activate hypertrophic chondrocyte gene expression. *Dev. Dyn.* **236,** 1954–1962
20. Kobayashi, T., Lyons, K. M., McMahon, A. P., and Kronenberg, H. M. (2005) BMP signaling stimulates cellular differentiation at multiple steps during cartilage development. *Proc. Natl. Acad. Sci. U.S.A.* **102,** 18023–18027
21. Scotti, C., Tonnarelli, B., Papadimitropoulos, A., Scherberich, A., Schaeren, S., Schauerte, A., Lopez-Rios, J., Zeller, R., Barbero, A., and Martin, I. (2010) Recapitulation of endochondral bone formation using human adult mesenchymal stem cells as a paradigm for developmental engineering. *Proc. Natl. Acad. Sci. U.S.A.* **107,** 7251–7256
22. Pullig, O., Weseloh, G., Ronneberger, D., Käkönen, S., and Swoboda, B. (2000) Chondrocyte differentiation in human osteoarthritis: expression of osteocalcin in normal and osteoarthritic cartilage and bone. *Calcif. Tissue Int.* **67,** 230–240
23. Sandell, L. J., and Aigner, T. (2001) Articular cartilage and changes in arthritis. An introduction: cell biology of osteoarthritis. *Arthritis Res.* **3,** 107–113
24. Dreier, R. (2010) Hypertrophic differentiation of chondrocytes in osteoarthritis: The developmental aspect of degenerative joint disorders. *Arthritis Res. Ther.* **12,** 216
25. Nelea, V., Luo, L., Demers, C. N., Antoniou, J., Petit, A., Lerouge, S., R Wertheimer, M., and Mwale, F. (2005) Selective inhibition of type X collagen expression in human mesenchymal stem cell differentiation on polymer substrates surface-modified by glow discharge plasma. *J. Biomed. Mater. Res. A* **75,** 216–223
26. Sekiya, I., Vuoristo, J. T., Larson, B. L., and Prockop, D. J. (2002) *In vitro* cartilage formation by human adult stem cells from bone marrow stroma defines the sequence of cellular and molecular events during chondrogenesis. *Proc. Natl. Acad. Sci. U.S.A.* **99,** 4397–4402
27. Imamura, T., Takase, M., Nishihara, A., Oeda, E., Hanai, J., Kawabata, M., and Miyazono, K. (1997) Smad6 inhibits signalling by the TGF-β superfamily. *Nature* **389,** 622–626
28. Zhu, H., Kavsak, P., Abdollah, S., Wrana, J. L., and Thomsen, G. H. (1999) A SMAD ubiquitin ligase targets the BMP pathway and affects embryonic pattern formation. *Nature* **400,** 687–693
29. Murakami, G., Watabe, T., Takaoka, K., Miyazono, K., and Imamura, T. (2003) Cooperative inhibition of bone morphogenetic protein signaling by Smurf1 and inhibitory Smads. *Mol. Biol. Cell* **14,** 2809–2817
30. Kawamura, I., Maeda, S., Imamura, K., Setoguchi, T., Yokouchi, M., Ishidou, Y., and Komiya, S. (2012) SnoN suppresses maturation of chondrocytes by mediating signal cross-talk between transforming growth factor-β and bone morphogenetic protein pathways. *J. Biol. Chem.* **287,** 29101–29113
31. Obeid, L. M., Linardic, C. M., Karolak, L. A., and Hannun, Y. A. (1993) Programmed cell death induced by ceramide. *Science* **259,** 1769–1771
32. Sjöholm, A. (1995) Ceramide inhibits pancreatic β-cell insulin production and mitogenesis and mimics the actions of interleukin-1 β. *FEBS Lett.* **367,** 283–286
33. Mebarek, S., Komati, H., Naro, F., Zeiller, C., Alvisi, M., Lagarde, M., Prigent, A. F., and Némoz, G. (2007) Inhibition of *de novo* ceramide synthesis upregulates phospholipase D and enhances myogenic differentiation. *J. Cell Sci.* **120,** 407–416
34. Sharma, K., and Shi, Y. (1999) The yins and yangs of ceramide. *Cell Res.* **9,** 1–10
35. Aubin, I., Adams, C. P., Opsahl, S., Septier, D., Bishop, C. E., Auge, N., Salvayre, R., Negre-Salvayre, A., Goldberg, M., Guénet, J. L., and Poirier, C.

(2005) A deletion in the gene encoding sphingomyelin phosphodiesterase 3 (Smpd3) results in osteogenesis and dentinogenesis imperfecta in the mouse. *Nat. Genet.* **37,** 803–805
36. Khavandgar, Z., Poirier, C., Clarke, C. J., Li, J., Wang, N., McKee, M. D., Hannun, Y. A., and Murshed, M. (2011) A cell-autonomous requirement for neutral sphingomyelinase 2 in bone mineralization. *J. Cell Biol.* **194,** 277–289
37. Stoffel, W., Jenke, B., Blöck, B., Zumbansen, M., and Koebke, J. (2005) Neutral sphingomyelinase 2 (smpd3) in the control of postnatal growth and development. *Proc. Natl. Acad. Sci. U.S.A.* **102,** 4554–4559
38. Stoffel, W., Jenke, B., Holz, B., Binczek, E., Günter, R. H., Knifka, J., Koebke, J., and Niehoff, A. (2007) Neutral sphingomyelinase (SMPD3) deficiency causes a novel form of chondrodysplasia and dwarfism that is rescued by Col2A1-driven smpd3 transgene expression. *Am. J. Pathol.* **171,** 153–161
39. Chae, Y. M., Heo, S. H., Kim, J. Y., Lee, J. M., Ryoo, H. M., and Cho, J. Y. (2009) Upregulation of smpd3 via BMP2 stimulation and Runx2. *BMB Rep.* **42,** 86–90
40. Atsumi, T., Miwa, Y., Kimata, K., and Ikawa, Y. (1990) A chondrogenic cell line derived from a differentiating culture of AT805 teratocarcinoma cells. *Cell Differ. Dev.* **30,** 109–116
41. Goldring, M. B., Birkhead, J. R., Suen, L. F., Yamin, R., Mizuno, S., Glowacki, J., Arbiser, J. L., and Apperley, J. F. (1994) Interleukin-1 β-modulated gene expression in immortalized human chondrocytes. *J. Clin. Invest.* **94,** 2307–2316
42. Alvarez, J., Sohn, P., Zeng, X., Doetschman, T., Robbins, D. J., and Serra, R. (2002) TGFβ2 mediates the effects of hedgehog on hypertrophic differentiation and PTHrP expression. *Development* **129,** 1913–1924
43. Shukunami, C., Ohta, Y., Sakuda, M., and Hiraki, Y. (1998) Sequential progression of the differentiation program by bone morphogenetic protein-2 in chondrogenic cell line ATDC5. *Exp. Cell Res.* **241,** 1–11
44. Yao, Y., and Wang, Y. (2013) ATDC5: an excellent *in vitro* model cell line for skeletal development. *J. Cell. Biochem.* **114,** 1223–1229
45. Origuchi, N., Ishidou, Y., Nagamine, T., Onishi, T., Matsunaga, S., Yoshida, H., and Sakou, T. (1998) The spatial and temporal immunolocalization of TGF-β 1 and bone morphogenetic protein-2/-4 in phallic bone formation in inbred Sprague Dawley male rats. *In Vivo* **12,** 473–480
46. Heinonen, J., Taipaleenmäki, H., Roering, P., Takatalo, M., Harkness, L., Sandholm, J., Uusitalo-Järvinen, H., Kassem, M., Kiviranta, I., Laitala-Leinonen, T., and Säämänen, A. M. (2011) Snorc is a novel cartilage specific small membrane proteoglycan expressed in differentiating and articular chondrocytes. *Osteoarthritis Cartilage* **19,** 1026–1035
47. Korchynskyi, O., and ten Dijke, P. (2002) Identification and functional characterization of distinct critically important bone morphogenetic protein-specific response elements in the Id1 promoter. *J. Biol. Chem.* **277,** 4883–4891
48. Lefebvre, V., Li, P., and de Crombrugghe, B. (1998) A new long form of Sox5 (L-Sox5), Sox6 and Sox9 are coexpressed in chondrogenesis and cooperatively activate the type II collagen gene. *EMBO J.* **17,** 5718–5733
49. Marchesini, N., Luberto, C., and Hannun, Y. A. (2003) Biochemical properties of mammalian neutral sphingomyelinase 2 and its role in sphingolipid metabolism. *J. Biol. Chem.* **278,** 13775–13783
50. Qin, J., Berdyshev, E., Poirer, C., Schwartz, N. B., and Dawson, G. (2012) Neutral sphingomyelinase 2 deficiency increases hyaluronan synthesis by up-regulation of hyaluronan synthase 2 through decreased ceramide production and activation of Akt. *J. Biol. Chem.* **287,** 13620–13632
51. Rokutanda, S., Fujita, T., Kanatani, N., Yoshida, C. A., Komori, H., Liu, W., Mizuno, A., and Komori, T. (2009) Akt regulates skeletal development through GSK3, mTOR, and FoxOs. *Dev. Biol.* **328,** 78–93
52. Shukunami, C., Shigeno, C., Atsumi, T., Ishizeki, K., Suzuki, F., and Hiraki, Y. (1996) Chondrogenic differentiation of clonal mouse embryonic cell line ATDC5 *in vitro*: differentiation-dependent gene expression of parathyroid hormone (PTH)/PTH-related peptide receptor. *J. Cell Biol.* **133,** 457–468
53. Matsumoto, K., Li, Y., Jakuba, C., Sugiyama, Y., Sayo, T., Okuno, M., Dealy, C. N., Toole, B. P., Takeda, J., Yamaguchi, Y., and Kosher, R. A. (2009) Conditional inactivation of Has2 reveals a crucial role for hyaluronan in skeletal growth, patterning, chondrocyte maturation and joint formation in the developing limb. *Development* **136,** 2825–2835
54. Ulici, V., Hoenselaar, K. D., Gillespie, J. R., and Beier, F. (2008) The PI3K pathway regulates endochondral bone growth through control of hypertrophic chondrocyte differentiation. *BMC Dev. Biol.* **8,** 40
55. Fujita, T., Azuma, Y., Fukuyama, R., Hattori, Y., Yoshida, C., Koida, M., Ogita, K., and Komori, T. (2004) Runx2 induces osteoblast and chondrocyte differentiation and enhances their migration by coupling with PI3K-Akt signaling. *J. Cell Biol.* **166,** 85–95
56. Kang, M. H., Kim, J. S., Seo, J. E., Oh, S. C., and Yoo, Y. A. (2010) BMP2 accelerates the motility and invasiveness of gastric cancer cells via activation of the phosphatidylinositol 3-kinase (PI3K)/Akt pathway. *Exp. Cell Res.* **316,** 24–37
57. Bartke, N., and Hannun, Y. A. (2009) Bioactive sphingolipids: metabolism and function. *J. Lipid Res.* **50,** S91–S96
58. Mora, A., Sabio, G., Risco, A. M., Cuenda, A., Alonso, J. C., Soler, G., and Centeno, F. (2002) Lithium blocks the PKB and GSK3 dephosphorylation induced by ceramide through protein phosphatase-2A. *Cell. Signal.* **14,** 557–562
59. Kolesnick, R., and Hannun, Y. A. (1999) Ceramide and apoptosis. *Trends Biochem. Sci.* **24,** 224–225
60. Wiesner, D. A., Kilkus, J. P., Gottschalk, A. R., Quintáns, J., and Dawson, G. (1997) Anti-immunoglobulin-induced apoptosis in WEHI 231 cells involves the slow formation of ceramide from sphingomyelin and is blocked by bcl-XL. *J. Biol. Chem.* **272,** 9868–9876
61. Lee, J. T., Xu, J., Lee, J. M., Ku, G., Han, X., Yang, D. I., Chen, S., and Hsu, C. Y. (2004) Amyloid-β peptide induces oligodendrocyte death by activating the neutral sphingomyelinase-ceramide pathway. *J. Cell Biol.* **164,** 123–131
62. Grassme, H., Jekle, A., Riehle, A., Schwarz, H., Berger, J., Sandhoff, K., Kolesnick, R., and Gulbins, E. (2001) CD95 signaling via ceramide-rich membrane rafts. *J. Biol. Chem.* **276,** 20589–20596
63. Dumitru, C. A., and Gulbins, E. (2006) TRAIL activates acid sphingomyelinase via a redox mechanism and releases ceramide to trigger apoptosis. *Oncogene* **25,** 5612–5625
64. Kultti, A., Kärnä, R., Rilla, K., Nurminen, P., Koli, E., Makkonen, K. M., Si, J., Tammi, M. I., and Tammi, R. H. (2010) Methyl-β-cyclodextrin suppresses hyaluronan synthesis by down-regulation of hyaluronan synthase 2 through inhibition of Akt. *J. Biol. Chem.* **285,** 22901–22910
65. Sabatini, M., Rolland, G., Léonce, S., Thomas, M., Lesur, C., Pérez, V., de Nanteuil, G., and Bonnet, J. (2000) Effects of ceramide on apoptosis, proteoglycan degradation, and matrix metalloproteinase expression in rabbit articular cartilage. *Biochem. Biophys. Res. Commun.* **267,** 438–444
66. Gilbert, S. J., Blain, E. J., Jones, P., Duance, V. C., and Mason, D. J. (2006) Exogenous sphingomyelinase increases collagen and sulphated glycosaminoglycan production by primary articular chondrocytes: an *in vitro* study. *Arthritis Res. Ther.* **8,** R89
67. Ehlert, K., Frosch, M., Fehse, N., Zander, A., Roth, J., and Vormoor, J. (2007) Farber disease: clinical presentation, pathogenesis and a new approach to treatment. *Pediatr. Rheumatol. Online J.* **5,** 15
68. Goldring, M. B. (1999) The role of cytokines as inflammatory mediators in osteoarthritis: lessons from animal models. *Connect. Tissue Res.* **40,** 1–11
69. Wiegmann, K., Schütze, S., Machleidt, T., Witte, D., and Krönke, M. (1994) Functional dichotomy of neutral and acidic sphingomyelinases in tumor necrosis factor signaling. *Cell* **78,** 1005–1015

Int J Clin Oncol (2013) 18:752–761
DOI 10.1007/s10147-013-0577-y

REVIEW ARTICLE

Lymph node micrometastasis in gastrointestinal tract cancer—a clinical aspect

Shoji Natsugoe · Takaaki Arigami · Yoshikazu Uenosono · Shigehiro Yanagita · Akihiro Nakajo · Masataka Matsumoto · Hiroshi Okumura · Yuko Kijima · Masahiko Sakoda · Yuko Mataki · Yasuto Uchikado · Shinichiro Mori · Kosei Maemura · Sumiya Ishigami

Received: 24 May 2013 / Published online: 18 June 2013

Abstract Lymph node micrometastasis (LNM) can now be detected thanks to the development of various biological methods such as immunohistochemistry (IHC) and reverse transcription-polymerase chain reaction (RT-PCR). Although several reports have examined LNM in various carcinomas, including gastrointestinal (GI) cancer, the clinical significance of LNM remains controversial. Clinically, the presence of LNM is particularly important in patients without nodal metastasis on routine histological examination (pN0), because patients with pN0 but with LNM already in fact have metastatic potential. However, at present, several technical obstacles are impeding the detection of LNM using methods such as IHC or RT-PCR. Accurate evaluation should be carried out using the same antibody or primer and the same technique in a large number of patients. The clinical importance of the difference between LNM and isolated tumor cells ($\leq$0.2 mm in diameter) will also be gradually clarified. It is important that the results of basic studies on LNM are prospectively introduced into the clinical field. Rapid diagnosis of LNM using IHC and RT-PCR during surgery would be clinically useful. Currently, minimally invasive treatments such as endoscopic submucosal dissection and laparoscopic surgery with individualized lymphadenectomy are increasingly being performed. Accurate diagnosis of LNM would clarify issues of curability and safety when performing such treatments. In the near future, individualized lymphadenectomy will develop based on the establishment of rapid, accurate diagnosis of LNM.

Keywords Lymph node metastasis · Micrometastasis · Esophageal cancer · Gastric cancer · Colorectal cancer

Introduction

One of the characteristics of malignant tumor is the ability to metastasize. If a tumor has high malignant potential, metastasis is often seen in wide areas. Thus, lymph node metastasis is one of the most important prognostic factors in various carcinomas, including gastrointestinal (GI) cancer. Even if complete lymph node dissection is performed in patients with early cancer, recurrent disease is sometimes encountered. Usually, histological examination for lymph node metastasis is performed using representative sections from the removed nodes. However, lymph node micrometastasis (LNM) may be identified in multiple sections of lymph nodes despite not being detected by routine histological examination using hematoxylin and eosin (HE) staining. Even in early gastric cancer, we found lymph node metastasis in 10.5 % of patients when additional sections of nodes were examined [1]. However, such procedures are labor-intensive and not cost-effective in active clinical practice.

The development of sensitive immunohistochemical techniques and reverse transcription-polymerase chain reaction (RT-PCR) has led to the detection of LNM that could not be found on routine histological examination. According to previous reports, cytokeratin (CK) AE1/AE3 and CAM5.2 monoclonal antibodies are often used for immunohistochemistry (IHC). Each technique has

S. Natsugoe (✉) · T. Arigami · Y. Uenosono · S. Yanagita · A. Nakajo · M. Matsumoto · H. Okumura · Y. Kijima · M. Sakoda · Y. Mataki · Y. Uchikado · S. Mori · K. Maemura · S. Ishigami
Department of Digestive Surgery, Breast and Thyroid Surgery, Kagoshima University Graduate School of Medical and Dental Sciences, 8-35-1 Sakuragaoka, Kagoshima 890-8520, Japan
e-mail: natsugoe@m2.kufm.kagoshima-u.ac.jp

specific advantages and disadvantages. Since IHC is relatively simple, the techniques are available in many institutions. However, problems arise in determining how many sections are sufficient for detection of LNM, the high cost of antibody, and false-positive results. On the other hand, RT-PCR offers an objective method for estimating LNM. Epithelial markers are usually available for detecting LNM, because epithelial components are not normally present in the lymph node. Although this approach offers high sensitivity, false-positive results are sometimes seen because of the presence of pseudogenes. Several epithelial markers can be used to recognize LNM in lymph nodes, but one of the key problems is determining what kind of marker is suitable for each carcinoma. Usually, CK, carcinoembryonic antigen (CEA) and squamous cell carcinoma-related antigen (SCC) are used for the detection of LNM.

This review focuses on the clinical significance of LNM detected by IHC and RT-PCR methods in carcinomas of the GI tract such as esophageal, gastric and colorectal cancer. Several reports have investigated LNM in specific lymph nodes such as recurrent nerve lymph nodes in esophageal cancer, para-aortic lymph nodes in gastric cancer, and lateral lymph nodes in colorectal cancer. Excluding those papers, we here review only reports in which LNM was examined in all dissected lymph nodes in GI cancer.

Definition of lymph node micrometastasis

Historically, several terms for tiny metastatic foci have been used, including occult metastasis, harbored metastasis, tumor microinvolvement and tumor deposit. Micrometastasis is currently defined according to the criteria of the tumor–node–metastasis (TNM) classification established by the International Union Against Cancer (UICC) in 2002, and is completely differentiated from isolated tumor cells (ITC) by size [2]. ITC represent either single tumor cells or small clusters of cells measuring $\leq$0.2 mm in greatest dimension and are commonly identified by IHC, but can be confirmed by routine HE staining. Moreover, ITC basically do not demonstrate evidence of metastatic activity, such as proliferation or stromal reaction, or penetration of vascular or lymphatic sinus walls. Patients with ITC in lymph nodes are staged as pN0 (i+). On the other hand, micrometastasis refers to tumor cell clusters measuring >0.2 mm but $\leq$2.0 mm in greatest dimension. Patients with micrometastasis in lymph nodes are staged as pN1 (mi). Furthermore, patients with node positivity as diagnosed by non-morphological findings using RT-PCR are staged as pN0 (mol+).

Lymph node micrometastasis in esophageal cancer

Several reports have investigated LNM detected by IHC in esophageal cancer (Table 1) [3–14]. The numbers of patients were relatively small, with all but two reports involving less than 100 patients. Two reports focused on T1 tumors, but the remaining reports covered advanced esophageal cancer. In Eastern countries, squamous cell carcinoma was a major histological type, while both squamous cell carcinoma and adenocarcinoma were included in Western countries. CK antibody (AE1/AE3) was commonly used for IHC. Single sections were used in 5 reports, and multiple sections in 7 reports. The definition of LNM varied. Seven authors defined LNM as identification of tumor cells in patients classified as pN0 according to routine HE staining. The remaining authors defined LNM by tumor size. The incidence of LNM ranged from 8.1 to 55.5 %. Since the diagnosis of LNM was based on morphology, this discrepancy might be due to the estimation of each author. Shiozaki et al. [11] conducted a multi-institutional study and the results of LNM were compared between institutional researchers and pathologists. Among 164 patients with pN0, 51 patients were diagnosed as micrometastasis-positive by institutional evaluation, but the pathologists identified only 25 patients as having micrometastasis-positive lymph nodes. Institutional positivity for micrometastasis was negated by these pathologists for the following reasons: (1) lack of nuclei in CK-positive cells; (2) location of stained cells outside the lymph node structure; or (3) stained cells appearing morphologically different from cancer cells or epithelial cells. If the evaluation of LNM detected by IHC differs between each institution, the results from different reports will naturally also be different. Common criteria for identifying LNM using IHC are thus necessary. Regarding the prognostic impact, 7 of 13 authors reported that the presence of LNM was related to poor prognosis. In particular, the two reports that included more than 100 cases both found significant differences in prognosis between the presence and absence of LNM [7, 11].

The relationship between LNM detected by RT-PCR and clinical significance was investigated in five studies (Table 2) [15–19]. Numbers of patients and numbers of examined nodes were not high. All reports included both early and advanced carcinoma. Two reports included only squamous cell carcinoma, two reports covered both squamous cell and adenocarcinoma and one report examined only adenocarcinoma. The primers for RT-PCR varied, including CEA, CK19, TACSTD-1, MUC1 and SCC. Double markers were used in two reports. The incidence of LNM ranged from 8.7 to 36.7 %, and all authors found a significant difference in prognosis between positive and negative LNM, with the single exception of a study that did

Table 1 Immunohistochemical studies in patients with histologically node-negative esophageal cancer diagnosed by hematoxylin–eosin staining

Years	Study	No. of patients	Average no. of LNs	Depth of invasion	Histological type	Method	Antibody	Sections for IHC	Definition of micrometastasis	No. of patients with micrometastases (%)	5-year survival (positive vs. negative)	*P*	Prognostic significance
1998	Natsugoe et al. [3]	41	–	T1–T3	SCC	IHC	CK (AE1/AE3)	Single	<0.5 mm	13 (31.7)	–	<0.05	Yes
1999	Glickman et al. [4]	78	7.4	–	SCC, AC	IHC	CK (AE1/AE3)	Multiple	≤2 mm	20 (25.6)	–	–	No
2000	Matsumoto et al. [5]	59	46.0	T1–T3	SCC	IHC	CK (AE1/AE3)	Single	pN0 by HE staining	39 (55.5)	44.6 vs. 91.0 %	0.002	Yes
2001	Sato et al. [6]	50	36.8	T1–T4	SCC	IHC	CK (AE1/AE3)	Single	pN0 by HE staining	20 (40.0)	78.0 vs. 75.0 %	0.91	No
2002	Komukai et al. [7]	104	74.7	T1–T3	SCC	IHC	CK (AE1/AE3)	Multiple	pN0 by HE staining	47 (45.2)	34.0 vs. 72.0 %	<0.01	Yes
2002	Nakamura et al. [8]	53	47.4	T1–T3	SCC	IHC	CK (AE1/AE3)	Single	pN0 by HE staining	14 (26.4)	–	0.16	No
2002	Doki et al. [9]	41	52.9	T3–T4	SCC	IHC	CK (AE1/AE3)	Single	pN0 by HE staining	11 (26.8)	28.0 vs. 79.0 %	0.0188	Yes
2003	Tanabe et al. [10]	46	–	Tl	SCC	IHC	CK (AE1/AE3)	Multiple	≤5 cells	12 (26.1)	–	–	No
2007	Shiozaki et al. [11]	167	–	T1–T3	SCC	IHC	CK (AE1/AE3)	Multiple	pN0 by HE staining	25 (15.0)	20.0 vs. 70 % (cluster)	0.0462	Yes
2009	Koenig et al. [12]	33	–	T1–T3	SCC, AC	IHC	CK (AE1/AE3)	Multiple	≤10 cells	3 (27.3)	30.0 vs. 76.0 %	0.009	Yes
2009	Zingg et al. [13]	86	14.0	T1–T3	SCC, AC	IHC	CK (Lu-5)	Multiple	≥0.2, ≤2 mm	7 (8.1)	35.7 vs. 61.1 %	n.s.	No
2012	Prenzel et al. [14]	48	28.0	Tl	SCC, AC	IHC	CK (AE1/AE3)	Multiple	pN0 by HE staining	7 (14.6)	57.0 vs. 79.0 %	0.002	Yes

Table 2 RT-PCR studies in patients with histologically node-negative esophageal cancer diagnosed by hematoxylin–eosin staining

Years	Study	No. of patients	Total no. of LNs	Depth of invasion	Histological type	Method	Markers	No. of patients with micrometastases (%)	5-year survival (positive vs. negative)	P	Prognostic significance
2001	Godfrey et al. [15]	30	387	T1–T3	SCC, AC	RT-PCR	CEA	11 (36.7)	–	<0.0001	Yes
2005	Xi et al. [16]	34	314	Tis–T3	AC	RT-PCR	CK19, TACSTD-1	5 (14.7)	–	0.0023	Yes
2007	Li et al. [17]	93	426	T1–T3	SCC	RT-PCR	MUC1	32 (34.4)	18.8 vs. 47.6 %	0.004	Yes
2011	Sun et al. [18]	82	501	T1–T3	SCC	RT-PCR	MUC1	23 (28.1)	21.7 vs. 62.7 %	0.0001	Yes
2013	Hagihara et al. [19]	46	–	T1–T2	SCC, AC	RT-PCR	CEA, SCC	4 (8.7)	–	–	–

not refer to prognosis. The RT-PCR method is more sensitive than IHC for detecting LNM because of the greater quantity of sample. However, several problems remain for RT-PCR examination. Since these epithelial markers are not specific for cancer, how many markers are necessary? What primers are suitable? If esophageal cancer-specific markers become available, the results of RT-PCR examinations will become more reliable.

Lymph node micrometastasis in gastric cancer

We collected 16 reports in which LNM was investigated by IHC for gastric cancer (Table 3) [20–35]. The definition of LNM varied. A few studies examined the incidence of ITC and micrometastasis classified on the basis of the TNM classification criteria for gastric cancer [30, 31, 34, 36]. LNM is basically defined as the presence of a single or small clusters of gastric tumor cells identified by IHC in lymph nodes classified as pN0 from HE staining. Table 3 summarizes studies reported since 1996 on LNM determined by IHC in patients with pN0 gastric cancer. Numbers of patients and average number of lymph nodes examined ranged from 34 to 308, and from 9.0 to 41.9, respectively. Seven reports included only early gastric cancer, while the others included both early and advanced cancer. All researchers used CK antibody to detect LNM, and several kinds of CKs such as CAM5.2, AE1/AE3 and MNF116 were used. The percentage of patients with LNM ranged from 10.0 to 36.0 %. Even in the 7 reports limited to early cancer, the incidence of LNM was found in the range of 10.0 to 31.8 %. This suggests that LNM has frequently already occurred in T1 tumor even if lymph node metastasis is not identified on routine histological examination. Prognosis was described in 14 of the 16 reports. Regarding the relationship between presence and absence of LNM and prognosis, nine authors found a significant correlation. The authors who did not find a correlation between LNM and prognosis indicated that standard gastrectomy with D2 lymphadenectomy was an appropriate treatment for gastric cancer, even in the presence of LNM determined by IHC [24]. In contrast, in a study of 160 gastric cancer patients with pT1N0 tumors, Cao et al. [34] recently reported LNM as one of the most important prognostic factors in multivariate survival analysis. When Yonemura et al. [30] focused on the clinical significance of ITC (single tumor cells or small clusters of cells measuring ≤0.2 mm by TNM classification), patients with ITC showed a significantly poorer prognosis than those without ITC. Furthermore, they examined immunohistochemically the proliferative activity of ITC using Ki-67 (MIB-1) and demonstrated positive MIB-1 labeling in 12 of 25 ITC (48.0 %) with a single tumor cell and in 49 of 52 ITC (94.2 %) with clusters. Similarly, when we assessed the proliferative activity of ITC and micrometastasis by double-staining IHC analysis with CY and Ki-67 mAb, Ki-67 positivity rates for LNM and ITC were 92 and 29 %, respectively [36]. These two studies suggest that, at the very least, micrometastatic tumor cells in lymph nodes display proliferative activity. Residual ITC when complete lymph node dissection is not performed might thus represent a high risk factor for tumor recurrence.

Some researchers have tried to examine LNM using RT-PCR (Table 4) [37–41]. According to these studies, simplex or multiplex RT-PCR assay using target molecular markers is performed for the detection of LNM in gastric cancer. The number of patients was relatively small, ranging from 10 to 80, and the markers used varied, including CEA, CK, Mage3, MUC2 and TFF1. The incidence of LNM detected by RT-PCR was over 20 %. We compared the incidence of LNM between IHC and RT-PCR assay in 1,862 lymph nodes obtained from 80 patients

Table 3 Immunohistochemical studies in patients with histologically node-negative gastric cancer diagnosed by hematoxylin–eosin staining

Years	Study	No. of patients	Average no. of LNs	Depth of invasion	Method	Antibody	No. of sections for IHC	Definition of micrometastasis	No. of patients with micrometastases (%)	5-year survival (positive vs. negative)	*P*	Prognostic significance
1996	Maehara et al. [20]	34	12.4	T1	IHC	CK (CAM5.2)	–	pN0 by HE staining	8 (23.5)	–	<0.05	Yes
2000	Cai et al. [21]	69	25.0	T1b	IHC	CK (CAM5.2)	Single	pN0 by HE staining	17 (24.6)	82.0 vs. 100.0 %	<0.01	Yes
2000	Harrison et al. [22]	25	9.0	T1–T4	IHC	CK (CAM5.2)	–	pN0 by HE staining	9 (36.0)	35.0 vs. 66.0 %	0.048	Yes
2001	Nakajo et al. [23]	67	26.3	T1–T3	IHC	CK (AE1/AE3)	Single	pN0 by HE staining	10 (14.9)	–	<0.05	Yes
2001	Fukagawa et al. [24]	107	41.9	T2–T3	IHC	CK (AE1/AE3)	Multiple	pN0 by HE staining	38 (35.5)	94.0 vs. 89.0 %	0.86	No
2001	Morgagni et al. [25]	139	10.7	T1	IHC	CK (MNF 116)	Multiple	pN0 by HE staining	24 (17.3)	87.0 vs. 88.0 %	0.6564	No
2002	Choi et al. [26]	88	25.8	T1b	IHC	CK (35βH11)	Single	pN0 by HE staining	28 (31.8)	92.9 vs. 95.0 %	0.6836	No
2002	Yasuda et al. [27]	64	31.9	T2–T4a	IHC	CK (CAM5.2)	Multiple	pN0 by HE staining	20 (31.3)	66.0 vs. 95.0 %	<0.01	Yes
2003	Morgagni et al. [28]	300	18.0	T1	IHC	CK (MNF 116)	Multiple	pN0 by HE staining	30 (10.0)	94.0 vs. 89.0 %	0.7797	No
2006	Miyake et al. [29]	120	29.1	T1	IHC	CK (AE1/AE3)	Multiple	≤0.2 mm	27 (22.5)	–	–	–
2007	Yonemura et al. [30]	308	39.0	T1–T4	IHC	CK (AE1/AE3)	–	≤0.2 mm	37 (12.0)	–	0.014	Yes
2008	Kim et al. [31]	184	27.1	T1–T4a	IHC	CK (AE1/AE3)	–	pN0 by HE staining	31 (16.8)	58.5 vs. 91.8 %	<0.001	Yes
2008	Ishii et al. [32]	35	29.4	T1b–T2	IHC	CK (O.N.352)	Multiple	pN0 by HE staining	4 (11.0)	–	–	–
2009	Kim et al. [33]	90	39.2	T1	IHC	CK (AE1/AE3)	–	≤2 mm	9 (10.0)	100 vs. 100 % (DSS)	–	No
2011	Cao et al. [34]	160	10.4	T1	IHC	CK (AE1/AE3)	–	pN0 by HE staining	34 (21.3)	55.9 vs. 92.9 %	<0.001	Yes
2011	Wang et al. [35]	191	22.0	T1–T3	IHC	CK (AE1/AE3)	Multiple	>0.2 and ≤2 mm	54 (28.3)	27.8 vs. 87.1 %	<0.001	Yes